Biochemistry

 Volume 36, Number 13 April 1, 1997

Accelerated Publications

Hydrogen Exchange/Electrospray Ionization Mass Spectrometry Studies of Substrate and Inhibitor Binding and Conformational Changes of *Escherichia coli* Dihydrodipicolinate Reductase†

Fang Wang, John S. Blanchard,* and Xue-jun Tang*,‡

Department of Biochemistry, Albert Einstein College of Medicine, 1300 Morris Park Avenue, Bronx, New York 10461

Received December 13, 1996; Revised Manuscript Received January 28, 1997⊗

ABSTRACT: *Escherichia coli* dihydrodipicolinate reductase is one of seven enzymes in the succinylase pathway of bacterial L-lysine biosynthesis. The binding of NADH, a substrate, and 2,6-pyridinedicarboxylate, an inhibitor, to the recombinant, overexpressed enzyme has been analyzed using hydrogen/deuterium exchange and electrospray ionization/mass spectrometry. NADH binding reduces the extent of deuterium exchange, as does the subsequent binding of 2,6-pyridinedicarboxylate. Pepsin digestion of the deuterated enzyme and enzyme−inhibitor complex coupled with liquid chromatography/mass spectrometry has allowed the identification of four peptides whose deuterium exchange slows considerably upon the binding of the substrate or inhibitor. Two of these peptides represent regions known or thought to bind NADH and 2,6-pyridinedicarboxylate. Two additional peptides are located at the interdomain hinge region and are proposed to be exchangeable in the "open", catalytically inactive, conformation but are nonexchangeable in the "closed", catalytically active conformation formed after NADH and 2,6-pyridinedicarboxylate binding and domain closure. These studies provide a clear example of a catalytically essential domain movement in this enzyme.

Amide hydrogen exchange has been used for over two decades as a probe of peptide and protein dynamics and structure (Englander et al., 1979; Englander & Kallenbach, 1984). While the mechanisms of such exchange reactions are still poorly understood, the rates at which specific amide hydrogens exchange appear to depend on solvent accessibility and the formation of specific hydrogen-bonding patterns to the amide hydrogen. For small proteins which are soluble, high-resolution ^{1}H NMR methods can measure the kinetics of individual amide hydrogen exchange once assignment of these resonances is complete (Wagner & Wüthrich, 1982; Roder et al., 1985). Such studies can provide detailed information about dynamic processes, including local protein unfolding and the identification of intermediates in protein folding. For larger proteins which are not accessible to study by ^{1}H NMR methods, the use of electrospray ionization/mass spectrometry has allowed amide hydrogen exchange studies of the whole protein to be performed (Katta & Chait, 1993). While allowing global changes in exchange properties to be assessed, the resolution of the method to identify individual residues or regions undergoing exchange was limited. The coupling of mass spectrometric methods with protease-catalyzed protein hydrolysis and HPLC separation at pH values where exchange was significantly slowed permitted the spatial resolution of mass spectrometric methods to be

† This work was supported by a BRSG grant from the Albert Einstein College of Medicine to X.T. and NIH Grant AI33696 to J.S.B. The purchase of the PE-SCIEX API III mass spectrometer was partially supported by a grant from the NIH (RR09113).

* Authors to whom correspondence may be addressed.

‡ Present address: Wyeth-Ayerst Research, 401 North Middletown Road, Pearl River, NY 10965.

⊗ Abstract published in *Advance ACS Abstracts,* March 1, 1997.

S0006-2960(96)03065-6 CCC: $14.00

Scheme 1: Reaction Catalyzed by Dihydrodipicolinate Reductase

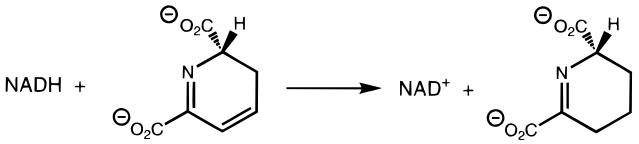

significantly extended (Zhang & Smith, 1993). This method has been applied to the study of amide hydrogen exchange in apo- and holomyoglobins (Johnson & Walsh, 1994; Wang & Tang, 1996), site-directed mutants of ferrocytochrome c_2 (Jaquinod et al., 1996), interactions of the Src homology 2 domain with ligands (Anderegg & Wagner, 1995), and the bacterial phosphocarrier protein (Johnson, 1996). Similar studies of rabbit muscle aldolase have allowed amide hydrogen exchange rates to be correlated with both intramolecular hydrogen bonding and crystallographic *B*-factors (Zhang et al., 1996).

The focus of the present study is *Escherichia coli* dihydrodipicolinate reductase, an enzyme of the L-lysine biosynthetic pathway. Bacteria synthesize lysine from L-aspartate via one of three pathways which share the first four, common steps. Aspartate is phosphorylated to yield aspartyl phosphate by aspartate kinase and then converted to aspartate semialdehyde by aspartate semialdehyde dehydrogenase. This compound undergoes an aldol condensation with pyruvate to generate the first unique lysine precursor, dihydrodipicolinate, by the action of dihydrodipicolinate synthase (Tamir & Gilvarg, 1974). Dihydrodipicolinate is reduced by NAD(P)H in the presence of dihydrodipicolinate reductase (DHPR) to generate tetrahydrodipicolinate (Scheme 1), the common precursor to the three pathways of lysine biosynthesis. The immediate precursor to L-lysine in all three pathways is the symmetric diamino acid, *meso*-diaminopimelate, a constituent of the peptidoglycan component of bacterial cell walls. The dual biosynthetic importance of these pathways, and the production of the common precursor tetrahydrodipicolinate by DHPR, has led us to suggest that this represents an appropriate target for inhibitor development. The *E. coli* enzyme has been cloned and sequenced (Bouvier et al., 1984), overexpressed and mechanistically characterized (Reddy et al., 1995), and crystallized and structurally characterized at 2.2 Å resolution (Scapin et al., 1995). The three-dimensional structure of the DHPR−NADPH complex revealed a two-domain protein, with the amino-terminal domain involved in nucleotide binding. The carboxyl-terminal domain is responsible for tetramerization and was additionally proposed to be the site of substrate binding on the basis of stereochemical arguments and sequence homologies between DHPR amino acid sequences from several bacteria (Scapin et al., 1995). This paper describes our studies to probe the global and regional conformational changes accompanying substrate (NADH) and inhibitor binding to DHPR using H/D exchange kinetics, protease fragmentation, and liquid chromatography/electrospray ionization/mass spectrometry (LC-ESI-MS).

MATERIALS AND METHODS

Materials. Recombinant *E. coli* dihydrodipicolinate reductase was expressed and purified as previously reported (Reddy et al., 1995). Pepsin and urea-d_4 were from Sigma, and 99.9 atom % D_2O was from Isotec, Inc. (Miamisburg, OH). All other chemicals and reagents were of the highest grade commercially available.

Exchange Studies. H/D exchange was initiated by diluting 2 μL of a 2.6 mM solution of DHPR in 25 mM Hepes, pH 7.8, in the presence or absence of NADH (2:1 molar ratio) and 2,6-pyridinedicarboxylate (20:1 molar ratio) into 38 μL of 25 mM Hepes, pD 7.8, in 99 atom % excess D_2O. 2,6-Pyridinedicarboxylate (PDC) is a competitive inhibitor of dihydrodipicolinate and exhibits an inhibition constant of *ca.* 25 μM (Reddy et al., 1995). Solutions were maintained at room temperature and allowed to exchange for various lengths of time. At appropriate intervals, aliquots of the DHPR solution were adjusted to pH 3 by the addition of an equal volume of 60 mM DCl and immediately cooled to 0 °C. Immediately after quenching, aliquots (5 μL) of the quenched solution were subjected to either LC-ESI-MS analysis or peptic digestion and subsequent LC-ESI-MS analysis to determine the extent of deuterium incorporation into DHPR or the peptic peptides.

Pepsin Digestion. Exchanged solutions of DHPR in the presence or absence of NADH and PDC were quenched and digested by adding 3 μL of these solutions to 37 μL of a solution containing 10 μM pepsin in 0.2 M ammonium phosphate, pH 2.5, containing 10% 20 mM DCl in 46 atom % excess D_2O and incubated for 2 min.

LC-ESI-MS Analysis of the Deuterated Enzyme and Its Peptic Peptides. LC-ESI-MS analysis of deuterated DHPR and its peptic peptides was performed to determine the extent of deuterium incorporation into DHPR and different regions of DHPR. A Shimadzu HPLC equipped with two LC-10AD pumps was used to pump the solvents at 50 μL/min and to generate acetonitrile gradients. The Rheodyne injector, column, and transfer line were immersed in an ice bath (0 °C) to minimize reverse exchange with the HPLC solvents. For the deuterated enzyme, aliquots (5 μL) of the exchanged and quenched solution were loaded onto a Vydac 1.0 × 150 mm C_4 column. After being desalted using a 7 min 0−10% acetonitrile gradient, the protein was eluted with a 5 min 10−90% acetonitrile gradient containing 0.01% trifluoroacetic acid (pH 2.7). For the peptic digests, 20 μL of the solution described above was injected onto a 1.0 × 250 mm Vydac C_8 column. After being desalted for 2 min at 5% acetonitrile, a 5 min 5−90% acetonitrile gradient containing 0.03% trifluoroacetic acid (pH 2.5) was used to elute and separate the peptides. The column effluent (50 μL/min) was delivered directly to the mass spectrometer without flow split. The mass resolution of the spectrometer was tuned to give a constant peak width of 1 Da (full width at half-maximum) across the mass range of interest. Full-scan mass spectra were acquired using a step size of 0.1 Da with a scan time of 4.25 s across the mass range of 1000−1650 for the protein sample and with a scan time of 2.97 s across the mass range of 400−1140 for the peptic digests.

The percentage of deuterium in peptide amide positions in DHPR or DHPR-derived peptic peptides was determined from the mass difference between nondeuterated and deuterated samples after correction for the loss of deuterium during LC-ESI-MS analysis or peptic digestion and subsequent LC-ESI-MS analysis (Zhang & Smith, 1993). Equation 1 was used for the calculation of the percentage of

$$\% \, D = (m_t - m_0)/(m_{100} - m_0) \times 100 \qquad (1)$$

deuterium incorporation, where m_t is the protein (peptide) mass at time t, m_0 is the protein mass at time zero, and m_{100} is the protein mass at infinite time (completely exchanged). All of the masses used in eq 1 are experimental masses measured by LC-ESI-MS. Completely deuterated DHPR was obtained by denaturing the enzyme in D_2O containing 8 M urea-d_4 and allowing exchange for 4 h at 22 °C. The urea-d_4 was removed prior to ESI-MS by centrifugal filtration of the aqueous solutions using ultrafree MC filters with a 10 000 Da molecular mass cutoff (Millipore). The number of deuteriums incorporated was determined by comparing the mass of the nonexchanged and fully exchanged protein using ESI-MS. The fully exchanged DHPR was digested with pepsin, and the back-exchange of each peptic peptide was determined from the theoretical mass for the completely amide-deuterated fragment and the experimental mass determined after LC-ESI-MS analysis. The extent of back-exchange varies between 30% and 60% during peptic digestion and LC-ESI-MS analysis.

Mass Spectrometry and Tandem Mass Spectrometry. All mass spectra were acquired using an API-III triple quadrupole mass spectrometer equipped with an atmospheric pressure ionization (API) source and a pneumatically assisted electrospray interface (PE-SCIEX, Thornhill, ON, Canada). High purity nitrogen was used as the nebulizing gas to prevent back-exchange of deuterium by laboratory air during the ion spray process. A Macintosh Quadra 950 was used for instrument control, data acquisition, and processing. Tandem mass spectrometry (MS/MS) was performed to identify peptic peptides. Fragment ion (tandem) mass spectra were obtained using collision-induced dissociation of precursor ions selected by their m/z value in the first quadrupole. Collisional activation was accomplished by introducing argon into the second (rf only) quadrupole, and the resulting fragment ions were analyzed in the third quadrupole. Optimum collision conditions varied with the precursor peptide, with target gas thickness ranging from $(1.5-4) \times 10^{14}$ atoms/cm^2 and accelerating potential differences into the collision cell in the range of 20−80 eV.

RESULTS AND DISCUSSION

The *E. coli dapB* gene encodes the 273 amino acid dihydrodipicolinate reductase. The enzyme catalyzes the NAD(P)H-dependent reduction of the α,β-unsaturated cyclic imine, dihydrodipicolinate, to form tetrahydrodipicolinate (Scheme 1). This compound serves as a precursor for each of the three pathways present in bacteria for the biosynthesis of diaminopimelate and L-lysine. The *E. coli* enzyme exhibits broad nucleotide selectivity and binds NADH six times more tightly than NADPH (K_d = 0.26 vs 1.8 μM; Reddy et al., 1995). The enzyme exhibits an ordered kinetic mechanism with reduced pyridine nucleotide binding before dihydrodipicolinate (DHP). 2,6-Pyridinedicarboxylate (PDC), the aromatic analog of DHP, is a 26 μM competitive inhibitor versus DHP and binds to the E−NADH complex. The three-dimensional crystal structure of the enzyme−NADPH complex has been solved and refined to 2.2 Å, and a potential DHP/PDC binding site was proposed from considerations of stereochemistry and electrostatics (Scapin et al., 1995). The present study was initiated to probe the potential of ESI-MS, coupled with protease fragmentation and HPLC, to define the DHP/PDC binding site, using hydrogen/deuterium exchange.

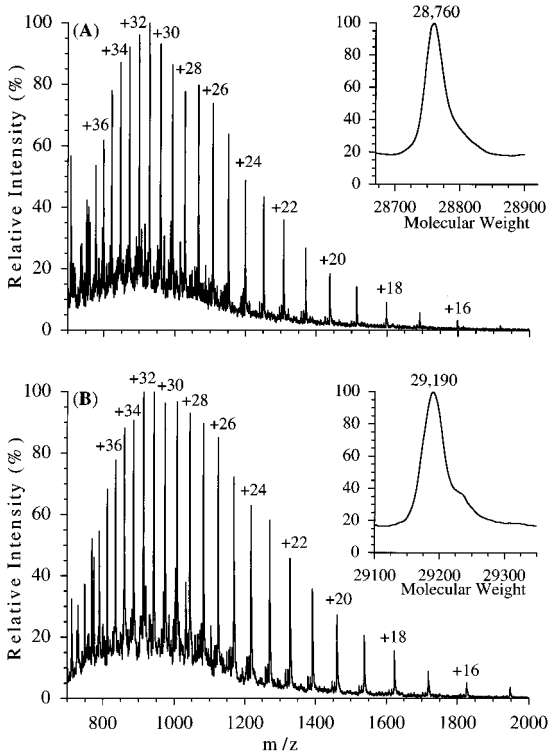

FIGURE 1: ESI mass spectra with deconvoluted spectra (insets) of *E. coli* DHPR in H_2O (A) and completely deuterated DHPR (B).

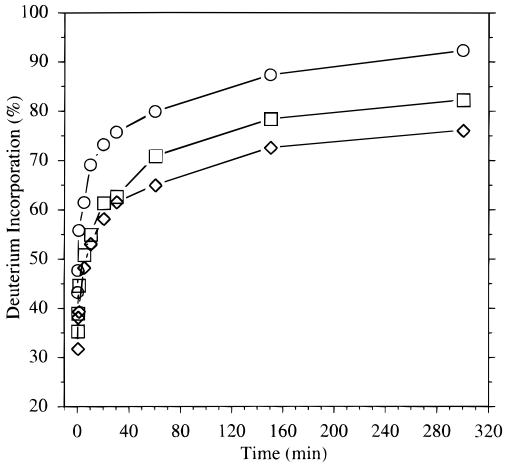

FIGURE 2: Percentage of deuterium at peptide amide positions as a function of time in DHPR alone (circles) and in DHPR in the presence of either a 2-fold molar excess of NADH (squares) or a 2-fold molar excess of NADH and a 20-fold molar excess of 2,6-pyridinedicarboxylate (diamonds).

Completely deuterated DHPR could not be obtained using elevated temperatures (70 °C), presumably due to its large size and tetrameric quaternary structure (Scapin et al., 1995). Denaturation in 8 M urea in 95 atom % excess D_2O allowed the essentially fully deuterated DHPR to be obtained, with a mass 430 Da higher than the nonexchanged protein (Figure 1: DHPR 28 760 vs DHPR-*d* 29 190). This compares to the mass difference predicted from the amino acid sequence of 461 resulting from the complete exchange of 269 amide hydrogens, 189 side-chain hydrogens, and the 3 amino terminal hydrogens, suggesting 93.3% deuteration. The completely deuterated DHPR was used as a control to calculate deuterium loss during pepsin digestion and LC-MS analysis of deuterated DHPR. H/D exchange was analyzed for DHPR incubated in 25 mM Hepes buffer, pD

Molecular weight	Fragment	Sequence
1429.68	[D] 68- 79 [T]	AVKDDFDVFIDF
1429.69	[F] 107- 120 [I]	DEAGKQAIRDAAAD
1430.84	[V] 136- 148 [D]	MLKLLEKAAKVMG

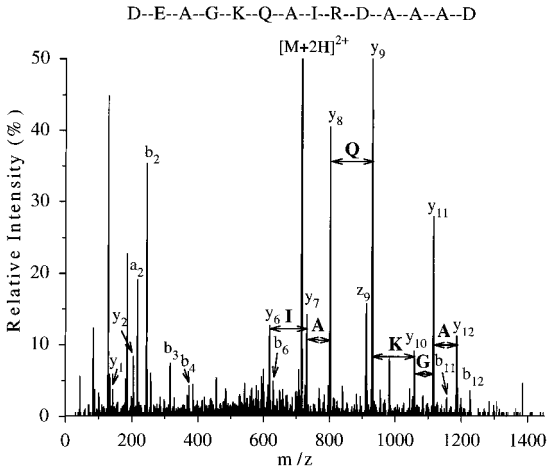

FIGURE 3: MS/MS spectrum of the doubly protonated peptic peptide ($[M + 2H]^{2+}$) representing residues 107−120 of DHPR. Some of the fragment ions have been labeled according to the nomenclature proposed by Biemann (1988).

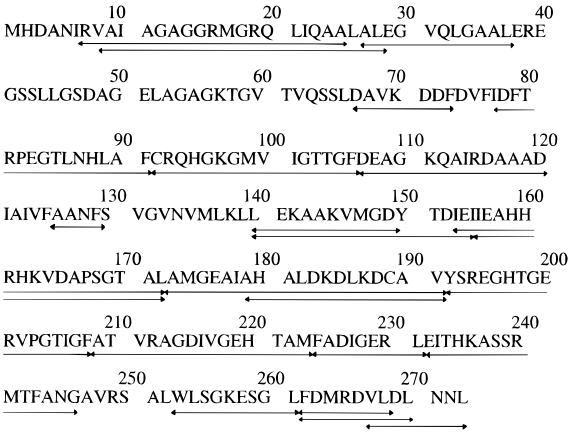

FIGURE 4: Amino acid sequence of DHPR indicating the position and sequence of peptic peptides evaluated in this study.

7.8, in the presence of either NADH or NADH and PDC, and the results shown in Figure 2 were obtained. The extent of H/D exchange into DHPR alone compared to the DHPR−NADH and DHPR−NADH−PDC complexes demonstrates the reduction of exchange rate in the binary and ternary complexes. Deuterium incorporation is reduced ∼10% in the DHPR−NADH binary complex and ∼15% in the DHPR−NADH−PDC ternary complex (error: <2%), compared to DHPR alone, suggesting that binding is preventing the exchange of either backbone or side-chain hydrogens in these complexes. In order to localize the regions of DHPR where exchange was prevented by substrate and inhibitor binding, we performed these experiments using pepsin digestion to generate peptides which could be individually analyzed and correlated with the known sequence and structure of the enzyme.

Pepsin cleaves proteins rather unpredictably, and therefore peptide mass alone is insufficient for the unambiguous determination of peptide identification. An example of this ambiguity, and its resolution, is demonstrated in Figure 3.

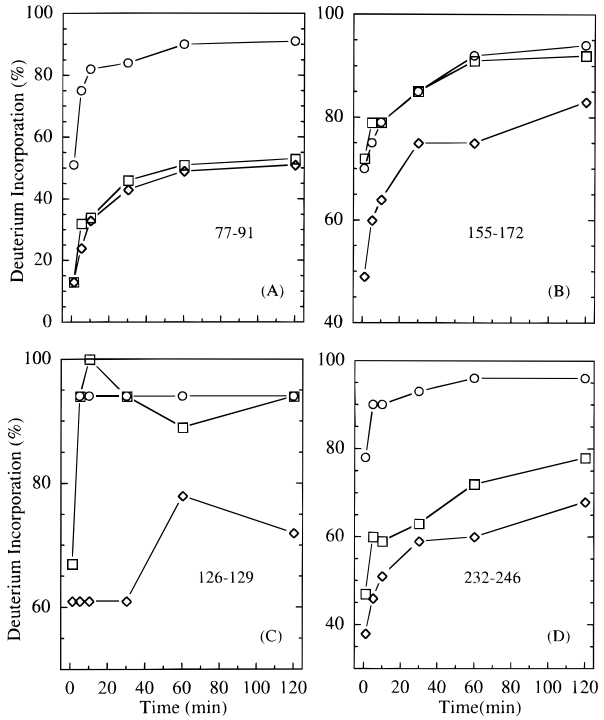

FIGURE 5: Percentage of deuterium at peptide amide positions as a function of time in peptides 77−91 (panel A), 155−172 (panel B), 126−129 (panel C), and 232−246 (panel D). In all panels, the exchanges have been determined for DHPR alone (circles) or for DHPR in the presence of either a 2-fold molar excess of NADH (squares) or a 2-fold molar excess of NADH and a 20-fold molar excess of 2,6-pyridinedicarboxylate (diamonds).

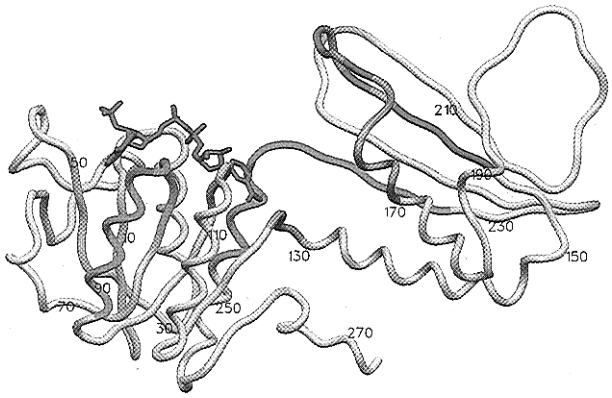

FIGURE 6: Structure of the *E. coli* DHPR−NADPH binary complex showing the bound NADPH in cyan. Conserved residues are highlighted in yellow, green, and orange. Residues in peptic peptides whose deuterium exchange is lower in the presence of NADH are shown in blue, while residues in peptic peptides whose deuterium exchange is lower in the presence of NADH and 2,6-pyridinedicarboxylate are shown in red.

Three peptides of molecular mass 1430 ± 1 Da could be generated by pepsin hydrolysis of DHPR, corresponding to residues 68−79, 107−120, and 136−148. The MS/MS spectrum of the HPLC-purified peptide obtained from pepsin digestion of DHPR is shown in Figure 3 and identified as corresponding to residues 107−120. Figure 4 shows the amino acid sequence of *E. coli* DHPR and illustrates the 22 peptides, representing 81% of the total protein sequence, used in this study to identify potential substrate and inhibitor binding regions. Most of these peptides exhibit essentially identical extents of deuterium exchange in the presence or absence of NADH or PDC. However, four peptides are discussed below which show significant differences in the

extent of exchange in the presence of NADH or NADH and PDC.

The peptide representing residues 77−91 shows a significant decrease in the extent of deuterium exchange in the presence of NADH (Figure 5, panel A), which is not affected by the presence of PDC. Examination of the three-dimensional structure of the DHPR−NADPH binary complex provides an explanation for this result. Residues 77−91 constitute portions of the fourth β strand and second α helix of the nucleotide binding domain, and side chains of Thr80 and Arg81 make hydrogen-bonding contacts with the nicotinamidyl 2′-ribose hydroxy and the pyrophosphate moiety of the bound nucleotide, respectively. Similar exchange behavior is exhibited by a peptide corresponding to residues 92−106 in the amino-terminal nucleotide binding domain (data not shown).

In contrast, deuterium exchange of the peptide representing residues 155−172 is not affected by the presence of NADH but is substantially reduced by the presence of PDC (Figure 5, panel B). This peptide is in a highly conserved region of DHPR, which because of the presence of a number of positively charged side-chain residues ($H_{159}HRHK_{163}$) was previously suggested (Scapin et al., 1995) to represent the substrate binding site. These data appear to confirm that original suggestion and argue that this loop between β strand 7 and α helix 5 binds the inhibitor and that inhibitor binding inhibits deuterium exchange.

Two other regions are noteworthy because of the effect of added NADH and PDC on the extent of their deuterium exchange. Peptides 126−129 and 232−246 (Figure 5, panels C and D) represent regions which connect the two domains of DHPR and include the "hinges" which have been previously discussed as important for domain movement (Ala_{127}−Ser_{130} and Ser_{239}−Arg_{240}). The reported structure for the DHPR−NADPH complex (Scapin et al., 1995) is in an "open", catalytically inactive conformation, based on the distance between the C4′ atom of bound NADPH and the modeled position of PDC. This distance would not permit the transfer of the hydride ion between the bound nucleotide and the C4 position of dihydrodipicolinate (Reddy et al., 1995), suggesting that after the ordered addition of reduced nucleotide and substrate (or inhibitor) a hinge movement (Gerstein et al., 1994) would be required to reorient the two domains into a catalytically active, "closed" conformation. The data presented in Figure 5 for the peptides representing these two hinge regions certainly support that proposal.

All of these data are graphically presented in Figure 6, where the peptide fragments whose deuterium exchange are affected by NADH and/or PDC binding in the structure of the DHPR−NADPH complex are color coded. We have highlighted regions which are identical in the sequences of seven bacterial DHPR's in yellow. Those residues which appear in peptide fragments which are exchanged to a lesser extent in the presence of NADH are shown in blue (77−91 and 232−246) and include conserved residues in the nucleotide binding domain (D78, T80, and P82, shown in green). Those residues which appear in peptide fragments which are exchanged to a lesser extent in the presence of PDC are shown in red (126−129 and 155−172) and include conserved residues in both the hinge region (A126 and F129) and the substrate binding domain (multiple residues shown in orange). Together, these data provide a dynamic picture of the changes which occur during the ordered addition of NADH and PDC (Reddy et al., 1995) and the conformational change accompanying domain movements. This technique should be broadly applicable to other systems, including substrate binding to enzymes and ligand binding to receptors, for which limited structural information is available.

ACKNOWLEDGMENT

The authors thank Dr. Giovanna Scapin (AECOM, Biochemistry) for preparing Figure 6 and Dr. Martin Pavelka (AECOM, Microbiology and Immunology) for providing unpublished results. We thank Mr. Edward Nieves for careful reading of the manuscript and helpful comments.

REFERENCES

Anderegg, R. J., & Wagner, D. S. (1995) *J. Am. Chem. Soc. 117*, 1374−1377.

Biemann, K. (1988) *Biomed. Environ. Mass Spectrom. 16*, 99−111.

Bouvier, J., Richaud, C., Richaud, F., Patte, J.-C., & Stragier, P. (1984) *J. Biol. Chem. 259*, 14829−14834.

Englander, J. J., Calhoun, D. B., & Englander, S. W (1979) *Anal. Biochem. 92*, 517−524.

Englander, S. W., & Kallenbach, N. R. (1984) *Q. Rev. Biophys. 16*, 521−655.

Gerstein, M., Lesk, A. M., & Chothia, C. (1994) *Biochemistry 33*, 6739−6749.

Jaquinod, M., Guy, P., Halgand, F., Caffrey, M., Fitch, J., Cusanovich, M., & Forest, E. (1996) *FEBS Lett. 380*, 44−48.

Johnson, R. S. (1996) *J. Am. Soc. Mass Spectrom. 7*, 515−521.

Johnson, R. S., & Walsh, K. A. (1994) *Protein Sci. 3*, 2411−2418.

Katta, V., & Chait, B. (1993) *J. Am. Chem. Soc. 115*, 6317−6321.

Reddy, S., Sacchettini, J. C., & Blanchard, J. S. (1995) *Biochemistry 34*, 3492−3501.

Roder, R., Wagner, G., & Wüthrich, K. (1985) *Biochemistry 24*, 7407−7411.

Scapin, G., Blanchard, J. S., & Sacchettini, J. C. (1995) *Biochemistry 34*, 3502−3512.

Tamir, H., & Gilvarg, C. (1974) *J. Biol. Chem. 249*, 3034−3040.

Wagner, G., & Wüthrich, K. (1982) *J. Mol. Biol. 160*, 343−361.

Wang, F., & Tang, X.-J. (1996) *Biochemistry 35*, 4069−4078.

Zhang, Z., & Smith, D. L. (1993) *Protein Sci. 2*, 522−531.

Zhang, Z., Post, C. B., & Smith, D. L. (1996) *Biochemistry 35*, 779−791.

BI963065G